HHS Public Access

Author manuscript

Biochim Biophys Acta Mol Basis Dis. Author manuscript; available in PMC 2025 January 01.

Published in final edited form as:

Biochim Biophys Acta Mol Basis Dis. 2024 January ; 1870(1): 166874. doi:10.1016/j.bbadis.2023.166874.

Inhibition of Wnt/β-catenin signaling reduces renal fibrosis in murine glycogen storage disease type Ia

Cheol Lee[a], **Kunal Pratap**[a], **Lisa Zhang**[a], **Hung Dar Chen**[a], **Sudeep Gautam**[a], **Irina Arnaoutova**[a], **Mahadevan Raghavankutty**[b], **Matthew F. Starost**[c], **Michael Kahn**[d], **Brian C. Mansfield**[a], **Janice Y. Chou**[a,*]

[a]Section on Cellular Differentiation, Division of Translational Medicine, *Eunice Kennedy Shriver* National Institute of Child Health and Human Development, National Institutes of Health, Bethesda, MD 20802, USA

[b]Section on Developmental Genetics, Division of Translational Medicine, *Eunice Kennedy Shriver* National Institute of Child Health and Human Development, National Institutes of Health, Bethesda, MD 20802, USA

[c]Division of Veterinary Resources, National Institutes of Health, Bethesda, MD 20802, USA

[d]Department of Cancer Biology and Molecular Medicine, Beckmann Research Institute, City of Hope, Duarte, CA 91010

Abstract

Glycogen storage disease type Ia (GSD-Ia) is caused by a deficiency in the enzyme glucose-6-phosphatase-α (G6Pase-α or G6PC) that is expressed primarily in the gluconeogenic organs, namely liver, kidney cortex, and intestine. Renal G6Pase-α deficiency in GSD-Ia is characterized by impaired gluconeogenesis, nephromegaly due to elevated glycogen accumulation, and nephropathy caused, in part, by renal fibrosis, mediated by activation of the renin-angiotensin system (RAS). The Wnt/β-catenin signaling regulates the expression of a variety of downstream mediators implicated in renal fibrosis, including multiple genes in the RAS. Sustained activation of Wnt/β-catenin signaling is associated with the development and progression of renal fibrotic lesions that can lead to chronic kidney disease. In this study, we examined the molecular mechanism underlying GSD-Ia nephropathy. Damage to the kidney proximal tubules is known to trigger acute kidney injury (AKI) that can, in turn, activate Wnt/β-catenin signaling. We

*Correspondence should be addressed to: Janice Y. Chou, Building 10, Room 8N-240C, NIH, 10 Center Drive, Bethesda, MD 20892-1830, Tel: 301-496-1094; Fax: 301-402-6035, chouja@mail.nih.gov.

Author contributions

CL performed the experiments, analyzed the data, and wrote the paper; KP, LZ, HDC, SG, IA, and MR performed the experiments, analyzed the data, and edited the manuscript; MFS performed pathological analysis and edited the manuscript; MK and BCM analyzed the data and edited the manuscript; JYC designed the research, acquired the funding, analyzed the data, wrote the paper, and is the GUARANTOR for the article.

Disclosure

CL, KP, LZ, HDC, SG, IA, MR, MFS, BCM, and JYC declare that they have no conflicts of interest.
MK is a co-founder and has an equity position in 3 + 2 Pharma.

show that GSD-Ia mice have AKI that leads to activation of the Wnt/β-catenin/RAS axis. Renal fibrosis was demonstrated by increased renal levels of Snail1, α-smooth muscle actin (α-SMA), and extracellular matrix proteins, including collagen-Iα1 and collagen-IV. Treating GSD-Ia mice with a CBP/β-catenin inhibitor, ICG-001, significantly decreased nuclear translocated active β-catenin and reduced renal levels of renin, Snail1, α-SMA, and collagen-IV. The results suggest that inhibition of Wnt/β-catenin signaling may be a promising therapeutic strategy for GSD-Ia nephropathy.

Graphical Abstract

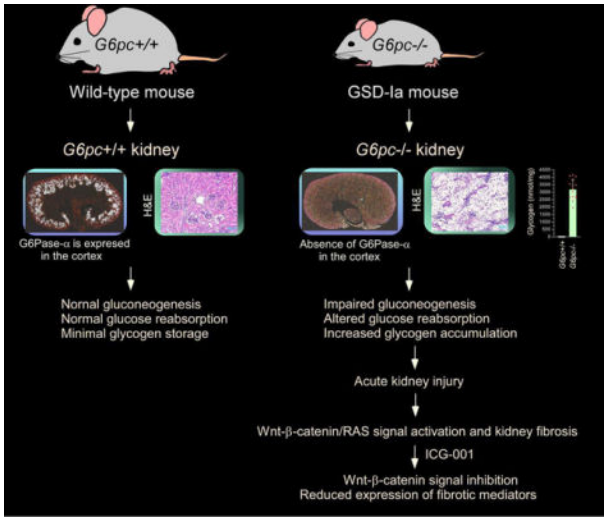

Keywords

Glucose-6-phosphatase-α; glucose reabsorption; acute kidney injury; nephromegaly; ICG-001

1. Introduction

Renal disease is a serious complication for glycogen storage disease type Ia (GSD-Ia, MIM232200), which is caused by a deficiency in glucose-6-phosphatase-α (G6Pase-α or G6PC) that is expressed primarily in the liver, kidney cortex, and intestine [1–3]. The early kidney manifestations of GSD-Ia are impaired renal gluconeogenesis and nephromegaly, caused by increased glycogen accumulation [1–3]. The only therapies currently available to treat GSD-Ia are dietary therapies [4–6] which have significantly alleviated metabolic abnormalities but only delay the onset of chronic kidney disease (CKD). The underlying pathological processes remain uncorrected, and glomerular hyperfiltration, hypercalciuria, hypocitraturia and urinary albumin excretion still occur in metabolically compensated GSD-Ia patients [1–3].

There is a long period of silent renal disease in GSD-Ia during which glomerular hyperfiltration is the only demonstrable renal abnormality [7,8]. This is followed by microalbuminuria, proteinuria, and ultimately, renal failure. Pathologically, GSD-Ia nephropathy exhibits interstitial fibrosis, tubular atrophy, and glomerulosclerosis with

marked glomerular basement-membrane thickening [7,8]. In many kidney diseases, tissue fibrosis is the result of excessive accumulation of extracellular matrix (ECM) proteins [9,10], which along with evolved interstitial fibrosis and glomerulosclerosis impairs renal function, leading to organ failure [9,10]. Using *G6pc*-deficient (*G6pc*−/−) mice that recapitulate the phenotype of human GSD-Ia [11], we have shown that fibrosis is also one mechanism underlying GSD-Ia nephropathy, mediated by upregulation of the renin-angiotensin system (RAS) [12].

The Wnt/β-catenin signaling pathway controls the expression of a variety of downstream mediators implicated in kidney fibrosis [13–16], including multiple genes in the RAS [13]. In the canonical Wnt/β-catenin pathway, Wnt interacts with the cell-surface receptors Frizzled and LRP5/6 (low-density lipoprotein receptor-related protein-5/6), leading to dephosphorylation and activation of β-catenin [13–16]. The activated β-catenin is translocated to the nucleus, where it binds to TCF/LEF (T-cell factor/lymphoid enhancer-binding factor), and recruits co-activators, such as CBP (CREB-binding protein) to form a transcriptionally active complex that promotes the transcription of Wnt target genes [13–16]. The Wnt/β-catenin pathway is usually suppressed during tissue homeostasis but can be activated during organ injury and regeneration, with sustained signaling activation promoting fibrosis [13–16]. Targeting Wnt/β-catenin signaling may be a promising therapeutic strategy for treating kidney disease.

Due to the severity of the disease, the *G6pc*−/− mice cannot be sustained beyond 6 weeks of age [11]. To study longer-term complications of GSD-Ia nephropathy, a mouse line that retains 50% of wild-type renal G6Pase-α activity allowing survival to adulthood has been described [17]. After age 6 months, this mouse strain presents with early renal perturbation, including increased expression of angiotensinogen, a component of the RAS, but renal levels of β-catenin were reportedly decreased [17]. In the current study, we examined the molecular mechanism underlying GSD-Ia nephropathy using two GSD-Ia mouse models, the global *G6pc*−/− and kidney-specific *G6pc*−/− mice, which both lack renal G6Pase-α activity. In contrast to the earlier study [17], we show that Wnt/β-catenin signaling is upregulated in GSD-Ia kidneys along with elevated expression of many proteins that mediate fibrosis.

G6Pase-α catalyzes the final step in glycogenolysis and gluconeogenesis, converting G6P to glucose [1–3]. However, the primary functional roles of G6Pase-α differ in the liver and kidney. The role of liver G6Pase-α is to maintain blood glucose homeostasis. During meals, excess blood glucose is taken up and stored in the liver as glycogen. When fasting, such as between meals and overnight, the liver produces endogenous glucose via glycogenolysis and gluconeogenesis to release 75–80% of the required blood glucose [18,19]. In contrast, the kidney stores little glycogen under physiological conditions. When fasting, the kidney primarily provides glucose via gluconeogenesis contributing 20–25% of blood glucose [18,19]. Overall, the kidneys are a glucose consumer, utilizing about 10% of all glucose consumed by the body in the post-absorptive state [18,19]. In the kidney, G6Pase-α is expressed primarily in the proximal tubular segment of the cortex [1,3,8], the site of gluconeogenesis. The kidney cortex is also responsible for urinary glucose reabsorption provided by the sodium-glucose cotransporters (SGLTs) and glucose transporters (GLUTs)

[20–22]. In acute kidney injury (AKI), a key trigger is proximal tubular damage [23] that can activate Wnt/β-catenin signaling [13–16]. We hypothesized that in GSD-Ia kidney, the stress incurred both by impaired gluconeogenesis and excessive glycogen accumulation elicits AKI, which activates Wnt/β-catenin signaling, leading to renal fibrosis.

ICG-001 is a small molecule that antagonizes Wnt/β-catenin signaling by competing with β-catenin for binding to CBP [24–26]. Studies using mouse models of Adriamycin nephropathy [13] and unilateral ureter obstruction [24] have shown that inhibiting Wnt/β-catenin signaling with ICG-001 represses RAS activation, ameliorates kidney fibrosis, and improves kidney function. Using GSD-Ia mice, we now show that in the presence of ICG-001, the amount of active β-catenin in the nucleus is significantly decreased, resulting in decreased renal levels of fibrotic mediators. These findings suggest that targeting Wnt/β-catenin signaling may be a valuable therapeutic for GSD-Ia nephropathy.

2. Material and methods

2.1. Animals

All animal studies were conducted under an animal protocol approved by the *Eunice Kennedy Shriver* National Institute of Child Health and Human Development Animal Care and Use Committee. The *G6pc*−/− mice [11] recapitulate the phenotype of human GSD-Ia, and their age-matched *G6pc*+/+ and *G6pc*+/− mice, which have a wild-type phenotype, were used as controls.

A G6PC-expressing recombinant adeno-associated virus serotype-2/8 vector (rAAV8-G6PC) [27] targets the liver but not the kidney [28] and can restore normalized liver function and glucose homeostasis in *G6pc*−/− mice [27,28]. Therefore, a GSD-Ia mouse model lacking kidney G6Pase-α activity (K-*G6pc*−/−) was generated by treating 2-day-old *G6pc*−/− mice with 10^{12} vg/kg of rAAV8-G6PC. The resulting K-*G6pc*−/− mice survive to adulthood without hypoglycemic seizures.

Three-day-old K-*G6pc*−/− mice were treated with ICG-001 at 500 μg/day, via intraperitoneal injection, for 18 consecutive days and phenotype assessed at age 3 weeks.

2.2. Renal metabolite analysis, hematoxylin & eosin, Oil Red O, and Masson's trichrome staining

Mouse kidneys were homogenized in 5% NP-40, incubated at 99°C for 5 min, and centrifuged to remove insoluble materials. The resulting supernatants were used to measure levels of G6P, lactate, triglyceride, and glycogen using the respective assay kits from BioVision (Milpitas, CA).

Hematoxylin & eosin (H&E) and Masson's trichrome staining were performed on paraffin-embedded mouse kidney sections. Oil Red O staining was performed on cryopreserved OCT embedded kidney sections. The stained sections were visualized using the Imager A2m microscope with Axiocam 506 camera and the ZEN 2.6 software (Carl Zeiss, White Plains, NY).

2.3. Western-blot analysis

Western-blot images were detected using the LI-COR Odyssey scanner and analyzed using the Image studio 3.1 software (Li-Cor Biosciences, Lincoln, NE). The antibodies used were: Abcam (Cambridge, MA), CTGF (ab6992); Cell Signaling Technology (Danvers, MA), rabbit β-actin (#4970), β-catenin (#8480), non-phospho β-catenin (#8814), αSMA (#14968), E-cadherin (#3195), N-cadherin (#13116), Snail1 (#3879), and collagen-Iα1 (#72026); Immuno-Biological Laboratories (Minneapolis, MN, USA), Angiotensinogen (28101); LS Bio (Seattle, WA, USA), collagen-IV (LS-B8763); Millipore Sigma (Burlington, MA, USA), ATP6AP2 (PRR) (HPA003156); MyBioSource (San Diego, CA); Dkk3 (MBS840225) and SGLT2 (MBS821113); Santa Cruz Biotechnology (Dallas, TX), mouse β-actin (sc-47778) and renin (sc-133145); Thermo Fisher Scientific (Waltham, MA), GLUT2 (720238).

2.4. Immunohistochemical analysis

Immunohistochemical analysis was performed on paraffin-embedded mouse kidney sections. The antibodies used were: Abcam, CTGF (ab6992); Cell Signaling Technology, non-phospho (active) β-Catenin (#8814) and αSMA (#19245); LS Bio, collagen-IV (LS-B8763), Snail1 (LS-B7247) and GLUT2 (LS-C498041); MyBioSource, Dkk3 (MBS3014809); Novus Biologicals (Centennial, CO, USA), collagen-Iα1 (NBP1–30054). The kidney sections were scanned using Zeiss Axioscan Z1 (Dublin, CA, USA) or MoticEasyScan Infinity 60 (Motic, Emeryville, CA, USA).

2.5. Serum creatinine, cystatin C, and blood urea nitrogen

Serum creatinine was determined using the Mouse Creatinine Assay Kit (# MBS763433) from MyBioSource (San Diego, CA), serum cystatin C was determined using the Mouse/Rat Cystatin C Quantikine ELISA Kit (# MSCTC0) from R&D Systems (Minneapolis, MN), and serum blood urea nitrogen (BUN) was determined using the Urea Nitrogen (BUN) Colorimetric Detection Kit (# EIABUN) from Thermo Fisher Scientific (Asheville, NC).

2.6. Statistical analysis

The unpaired t-test was performed using the GraphPad Prism Program, version 8 (GraphPad Software, San Diego, CA). Values were considered statistically significant at $p < 0.05$.

3. Results

3.1. G6pc−/− mice display a marked increase in renal glycogen accumulation

Like GSD-Ia patients, *G6pc*−/− mice are growth retarded and manifest nephromegaly and hepatomegaly caused by increased accumulation of glycogen and glycogen/neutral fat, respectively [1–3,11]. The body weight (BW) values of the *G6pc*−/− mice were 40–60% lower than those of their age-matched control mice during weeks 1 to 3 of postnatal development (Fig. 1A). Conversely, kidney weight (KW) and liver weight (LW) in *G6pc*−/− mice increased with the ratios KW/BW and LW/BW increasing 3- to 4-fold in the *G6pc*−/− mice, compared to the controls (Fig. 1A).

Under physiological conditions, the liver, but not the kidney, is the major organ that stores glycogen [18,19]. While renal glycogen contents averaged at ~2.0 nmol/mg at 1 to 3 weeks of age, hepatic glycogen contents averaged 90.6 ± 8.2, 136 ± 13.6, and 153.0 ± 31.4 nmol/mg, respectively in 1-, 2-, and 3-week-old control mice (Fig. 1B). During postnatal development of the *G6pc*−/− mice, glycogen contents increased markedly in both the kidney and the liver (Fig. 1B). Renal glycogen contents increased progressively in 1-, 2-, and 3-week-old *G6pc*−/− mice, averaging 825 ± 61.7, 1681 ± 153, and 3112 ± 230 nmol/mg, respectively (Fig. 1B). Hepatic glycogen contents in 1-, 2-, and 3-week-old *G6pc*−/− mice averaged 1221 ± 105.7, 1562 ± 213, and 530.0 ± 39.5 nmol/mg, respectively, peaking at age 2 weeks (Fig. 1B). Notably, in 3-week-old *G6pc*−/− mice, renal glycogen contents, estimated as nmol per mg liver protein, were 5.9-fold higher than that in the liver. H&E staining showed that the marked renal glycogen storage in the GSD-Ia kidneys resulted in enlargement of tubular cells and compression of the glomeruli (Fig. 1C).

G6Pase-α deficiency leads to G6P metabolic reprogramming and enhanced glycolysis [29]. At age 3 weeks, renal triglyceride levels were statistically similar between control and *G6pc*−/− mice (Fig. 1D). Compared to the controls, renal levels of G6P and lactate were significantly increased in *G6pc*−/− mice (Fig. 1D). Oil Red O staining showed that the kidneys of 3-week-old control and *G6pc*−/− mice displayed similarly low levels of neutral fat (Fig. 1C).

Renal function was assessed in 3-week-old *G6pc*−/− mice by measuring serum levels of creatinine, cystatin C, and BUN [30]. Compared to the control littermates, serum levels of creatinine and cystatin C were unchanged, but serum BUN levels were increased in the 3-week-old *G6pc*−/− mice (Fig. 1E).

3.2. G6pc−/− mice display altered renal glucose reabsorption

In addition to gluconeogenesis, renal proximal tubules also regulate glucose homeostasis via glucose reabsorption primarily by GLUT2 and SGLT2, expressed at the basolateral and apical membranes, respectively [20–22]. Compared to the controls, renal levels of GLUT2 that is responsible for majority of glucose release between cells and the bloodstream increased 3- to 7-fold in the *G6pc*−/− mice during weeks 1 to 3 of postnatal development (Fig. 2A). The increase in GLUT2 was observed in cytoplasm/brush border of renal tubules and mesangial cells of the glomeruli (Fig. 2B). Conversely, renal levels of SGLT2 that are responsible for over 90% of urinary glucose reabsorption decreased in the *G6pc*−/− mice from 73% of control levels at age 2 weeks to 47% of the control levels at age 3 weeks (Fig. 2A). Immunohistochemical analysis showed that renal levels of SGLT2 were significantly decreased in the proximal renal tubules of 3-week-old *G6pc*−/− mice, compared to age-matched controls (Fig. 2B).

3.3. G6pc−/− mice display AKI

Renal proximal tubules are particularly vulnerable to injury, and damage to the tubular segment of the nephron is a key mediator of AKI [23]. We hypothesized that the stress elicited by impaired gluconeogenesis, altered glucose reabsorption, and elevated glycogen accumulation could lead to AKI in *G6pc*−/− mice. E-cadherin and N-cadherin are cell

adhesion molecules that play crucial roles in epithelial cell integrity and polarity [31]. In human AKI and ischemic rat kidneys, E-cadherin immunostaining is unchanged while N-cadherin immunostaining is depleted [31]. While renal levels of E-cadherin were similar between control and *G6pc*−/− mice during postnatal development, renal levels of N-cadherin decreased progressively in *G6pc*−/− mice, beginning at age 1 week (Fig. 2C), suggesting the *G6pc*−/− mice suffer from AKI as early as 1-week-old.

Dickkopf-3 (Dkk3) is a secretory pro-fibrotic glycoprotein that is synthesized by stressed renal tubular epithelial cells [16,23,32]. The expression of Dkk3 correlates positively with AKI and is considered a marker for AKI. Dkk3 promotes epithelial-to-mesenchymal transition (EMT) and tubulointerstitial fibrosis by modulating the canonical Wnt/β-catenin signaling pathway [16,23,32]. Compared to the controls, renal levels of Dkk3 in *G6pc*−/− mice were elevated 4- to 8-fold during postnatal development (Fig. 3A). Immunohistochemical analysis of 1-week-old *G6pc*−/− and control mice showed the increase in Dkk3 in the *G6pc*−/− kidney was at the cytoplasm/brush border of renal tubules and epithelial cells of the collecting tubules (Fig. 3B), supporting an early onset of AKI in *G6pc*−/− mice.

Pro-renin receptor (PRR) is a ubiquitously expressed, transmembrane protein that can amplify Wnt/*β*-catenin signaling and promote fibrosis [33,34]. Compared to the controls, renal levels of PRR were similar between control and *G6pc*−/− (Fig. 3A), suggesting that PRR plays little role in *G6pc*−/− nephropathy.

Connective tissue growth factor (CTGF) is expressed at low levels in normal adult kidneys, whose expression increases significantly in tubular epithelial cell injury [35,36]. In progressive kidney diseases, CTGF plays an important role in the development of glomerulosclerosis and tubulointerstitial fibrosis [35,36]. Compared to the controls, renal levels of CTGF in *G6pc*−/− mice were elevated over 2-fold, beginning at age 1 week (Fig. 3A). Immunohistochemical analysis confirmed that CTGF was increased at renal proximal convoluted tubule membranes of 1-week-old *G6pc*−/− mice (Fig. 3B).

3.4. Induction of renal Wnt/β-catenin signaling in the G6pc−/− mice

In the canonical Wnt/β-catenin pathway, β-catenin is activated by dephosphorylation and translocation to the nucleus, where it forms a transcriptionally active complex with TCF/LEF and CBP or p300 that promotes the transcription of Wnt-targeted genes [14–16]. At age 1-week, renal levels of total and active β-catenin in the *G6pc*−/− mice were slightly elevated over the controls (Fig. 3C). At age 2 weeks, renal levels of total and active β-catenin in the *G6pc*−/− mice were 1.8-fold and 1.7-fold higher than their respective controls (Fig. 3C). Remarkedly, at age 3 weeks, renal levels of total and active β-catenin in the *G6pc*−/− mice were 5.1- and 6.7-fold over their controls, respectively (Fig. 3C). The increase in nuclear translocation of the active β-catenin was confirmed by immunohistochemistry as shown in Fig. 7A and 7B.

We have shown that one mechanism underlying GSD-Ia nephropathy is renal fibrosis mediated by upregulation of the RAS [12]. Wnt/β-catenin signaling positively regulates the transcription of multiple genes in the RAS [13] and the Wnt/β-catenin/RAS axis reinforces

kidney damage [13,14,37]. The rate-limiting step in RAS activation is the conversion of angiotensinogen (AGT) to angiotensin-I, catalyzed by renin [37]. Compared to the controls, renal levels of renin and AGT were increased by 1.8-fold and 1.9-fold, respectively in *G6pc*−/− mice at age 3 weeks (Fig. 4A).

Another target of Wnt/β-catenin signaling is the transcriptional factor Snail1 that plays a key role in fibroblast activation [38]. Activation of Snail1 triggers a partial EMT, leading to renal epithelial cell dedifferentiation and renal fibrosis [38]. Compared to the controls, renal levels of Snail1 were elevated 1.5- to 2-fold, beginning at age 2 weeks (Fig. 4B). Immunohistochemical analysis showed that the increase in renal Snail1 was observed at proximal convoluted tubules and collecting duct tubules of the G6pc−/− kidneys (Fig. 4C).

Renal fibrosis is characterized by fibroblast proliferation and differentiation to myofibroblasts. The myofibroblasts produce a signature protein, α-smooth muscle actin (α-SMA) [39,40] as well as ECM proteins, such as collagens [9,10]. Compared to the controls, renal levels of α-SMA were increased 2.1-fold at age 3 weeks (Fig. 4B). In the control kidney, α-SMA was found at the vasculature network but in the *G6pc*−/− kidney, the increase in α-SMA was observed in the vasculature network. the basement membranes of glycogen-laden proximal convoluted tubules, and the glomeruli (Fig. 4C).

Compared to the controls, renal levels of collagen I-α1 (Col-Iα1) were increased 2.8- to 3.2-fold and renal levels of Col-IV were increased 1.7- to 4.6-fold, both beginning at age 2 weeks (Fig. 5A). While the increase in Col-Iα1was seen at the interstitial and/or basement membranes of cortical tubules, the increase in Col- IV was observed at the proximal convoluted tubules, basement membranes, and mesangial cells of the glomeruli (Fig. 5B). Finally, interstitial fibrosis in the kidney of 3-week-old *G6pc*−/− mice was demonstrated by the blue colored staining of the collagen fibers by Masson's trichrome (Fig. 5C).

3.5. Generation of the kidney-specific G6pc knockout (K-G6pc−/−) mice

The *G6pc*−/− mice are unable to tolerate stress mediated by daily intraperitoneal injections because of their natural history of frequent, hypoglycemic seizures. To gain mechanistic insights of GSD-Ia nephropathy, we generated a new model for the study of renal disease, the K-*G6pc*−/− mice by treating 2-day-old global *G6pc*−/− mice with 10^{12} vg/kg of rAAV8-G6PC [27], that transduces the liver but not the kidney [28]. We showed that the resulting K-*G6pc*−/− mice expressed 1.5 units of hepatic G6Pase-α activity and nondetectable levels of renal G6Pase-α activity. To validate that renal dysfunction in the K-*G6pc*−/− mice mimicked that of the *G6pc*−/− mice, we examined the expression of genes involved in renal homeostasis and fibrosis in 3-week-old control, *G6pc*−/−, and K-*G6pc*−/− mice. Renal levels of GLUT2, SGLT2, N-cadherin, Dkk3, and CTGF were similar between *G6pc*−/− and K-*G6pc*−/− mice (Fig. 6A). Importantly, renal levels of total and active β-catenin, Snail1, renin, α-SMA, and Col-Iα1 were statistically similar between *G6pc*−/− and K-*G6pc*−/− mice (Fig. 6B), demonstrating that the K-*G6pc*−/− mice, lacking renal G6Pase-α activity, represent a valid model for studying GSD-Ia nephropathy.

3.6. ICG-001 inhibits Wnt/β-catenin signaling and reduces renal fibrosis

ICG-001 is a small molecule drug that antagonizes Wnt/β-catenin signaling by competing with β-catenin for binding to CBP [24–26]. Zhou et al [13] have shown that ICG-001 blocks RAS activation and ameliorates renal fibrosis in a mouse model of Adriamycin nephropathy. We treated 3-day-old K-*G6pc*−/− mice with daily intraperitoneal injections of 500 ug ICG-001 for 18 consecutive days. At age 3 weeks, immunohistochemical analysis using an antibody against the active β-catenin showed a diffused renal cytoplasmic β-catenin staining in the control mice but increased nuclear β-catenin staining in the renal cortex and medulla tubules of the K-*G6pc*−/− mice (Fig. 7A). Quantification analysis showed that nuclear β-catenin staining in the kidney of ICG-001-treated K-*G6pc*−/− mice was significantly decreased compared to that of the untreated K-*G6pc*−/− mice, although the staining remained higher than in the control mice (Fig. 7B). Accordingly, compared to the untreated K-*G6pc*−/− mice, the ICG-001-treated K-*G6pc*−/− mice expressed significantly reduced renal levels of renin, Snail1, α-SMA, and Col-IV (Fig. 7C). As expected, renal levels of Dkk3, SGLT2, or N-cadherin were statistically similar between 3-week-old untreated and ICG-001-treated K-*G6pc*−/− mice (Fig. 8A).

Nephromegaly, hepatomegaly, and the elevation of renal levels of G6P, lactate, and glycogen are direct metabolic consequences of G6Pase-α deficiency and the early clinical manifestations of GSD-Ia [1–3]. As expected, compared to the untreated K-*G6pc*−/− mice, the ICG-001-treated K-*G6pc*−/− mice displayed both nephromegaly and hepatomegaly (Fig. 8B). Moreover, renal levels of G6P, lactate, and glycogen were similarly elevated in untreated and ICG-001-treated K-*G6pc*−/− mice (Fig. 8C). Similarly, serum BUN levels remained high in both untreated and ICG-001-treated K-*G6pc*−/− mice (Fig 8D).

4. Discussion

GSD-Ia patients manifest nephropathy [1–3]. Pathological examinations of GSD-Ia patients with renal insufficiency have revealed interstitial fibrosis, tubular atrophy, and glomerulosclerosis with marked glomerular basement-membrane thickening [7,8]. Using *G6pc*−/− mice, we have shown that one mechanism underlying GSD-Ia nephropathy is renal fibrosis mediated by activation of the RAS [12]. We now show that impaired gluconeogenesis, altered glucose reabsorption, and elevated glycogen accumulation in *G6pc*−/− mice elicited AKI, leading to activation of the Wnt/β-catenin/RAS axis. Renal fibrosis was demonstrated by the increase in renal levels of Snail1, α-SMA, ECM proteins including Col-Iα1 and Col-IV, and confirmed by increased Masson's trichrome staining of collagen fibers. Importantly, treating K-*G6pc*−/− mice with ICG-001 [24–26], a specific CBP/β-catenin antagonist reduced renal levels of active nuclear β-catenin along with reduced renal levels of renin, Snail1, α-SMA, and Col-IV. Taken together, our results suggest that small molecule drugs that inhibit the interaction of *β*-catenin with CBP and prevent activation of Wnt/*β*-catenin target genes [26] might be a promising therapeutic approach to reduce renal fibrosis in GSD-Ia.

The primary consequence of a loss of G6Pase-α activity in GSD-Ia is a metabolic disturbance that leads to nephromegaly, hepatomegaly, and elevation of renal levels of G6P, lactate, and glycogen. As expected, inhibition of the Wnt/β-catenin/RAS axis with ICG-001

treatment did not impact nephromegaly, hepatomegaly, or the levels of metabolites in the kidney.

The most reliable early sign of renal dysfunction is the glomerular filtration rate measured using external filtration markers like FITC-inulin [41]. This technique was not applicable to the 3-week-old *G6pc*−/− mice due to their fragility. Instead, renal function was assessed by measuring serum levels of creatinine, cystatin C, and BUN [30]. Compared to the control littermates, serum levels of creatinine and cystatin C were unchanged, but serum BUN levels, which can be affected by physiological conditions not related to renal function [42], were increased in the 3-week-old *G6pc*−/− mice (Fig. 1E). Taken together, these data do not support evidence of an early-stage of renal dysfunction in 3-week-old *G6pc*−/− mice, which is consistent with the prognosis of human GSD-Ia where a long period of silent renal disease precedes the observable renal dysfunction [1–3].

The renal proximal tubules maintain glucose homeostasis through a combination of endogenous glucose production via gluconeogenesis [1–3] and glucose reabsorption via SGLTs and GLUT2 [20–22]. It has been well established that GSD-Ia kidneys lacking G6Pase-α manifest impaired gluconeogenesis [1–3]. Here we show that G6Pase-α-deficient kidney also displayed altered glucose reabsorption characterized by reduced levels of SGLT2, responsible for over 90% of urinary glucose reabsorption and increased levels of GLUT2, responsible for most of the glucose release into the blood stream. It has been shown that downregulation of SGLT2 protects the proximal tubule from further injury during AKI [22], suggesting the decrease in renal SGLT2 expression may be reno-protective. In diabetes mellitus, hyperglycemia increases glucose reabsorption through enhanced SGLT2 expression, and the SGLT2 inhibitors have become a mainstay to treat type 2 diabetes mellitus [20–22]. We speculate that upregulation of renal GLUT2 is a compensatory process to counter an absence of endogenous glucose production and reduced glucose reabsorption.

Under physiological conditions, in contrast to the liver, the kidney stores very little glycogen [18,19]. This is not the case for GSD-Ia where *G6pc*−/− mice manifest nephromegaly and hepatomegaly caused by excess accumulation of glycogen and glycogen/neutral fat, respectively [1–3,11]. During postanal development, the glycogen contents of both the kidney and the liver increase in the *G6pc*−/− mice. Significantly, in 3-week-old *G6pc*−/− mice, renal glycogen levels, estimated as nmol/mg, were ~6-fold higher than that in the liver. Accordingly, in the kidney of *G6pc*−/− mice the stress incurred by impaired gluconeogenesis, altered glucose reabsorption, and the marked increase in glycogen accumulation leads to reduced N-cadherin [31] and increased Dkk3 [16,23,32], both markers of AKI. Elevation of Dkk3 can promote Wnt/β-catenin signaling and accelerate renal fibrosis. The *G6pc*−/− kidney also displayed increased CTGF that can exert profibrotic effects through its interaction with LRP6 and activating Wnt/β-catenin signaling [35,36,43]. Importantly, the increase in Dkk3 and CTGF in *G6pc*−/− mice was observed at age 1 week, ahead of Wnt/β-catenin signaling activation. Taken together, activation of the Wnt/β-catenin/RAS axis along with enhanced expression of Dkk3 and CTGF is consistent with increased renal fibrosis in GSD-Ia.

Presently, angiotensin-converting enzyme (ACE) inhibitor therapy is recommended for GSD-I patients with early signs of nephropathy [3]. Two retrospective studies were undertaken to investigate the renoprotective effects of ACE inhibitors on GSD-Ia nephropathy [44,45]. The studies showed that ACE inhibitors significantly delayed the progression from glomerular hyperfiltration to microalbuminuria but the progression from microalbuminuria to proteinuria was not affected. Our results suggest that targeting Wnt/β-catenin signaling, which simultaneously inhibits multiple components of the RAS, should be better or at least equal to ACE inhibitor therapy. Future studies should also examine the roles of Dkk3 and CTGF in GSD-Ia nephropathy since they work synergistically with Wnt/β-catenin signaling to promote fibrosis.

While the *G6pc*−/− mice are a good model to study GSD-Ia nephropathy, these mice manifest severe hypoglycemia and cannot sustain stress, making mechanistic studies difficult. Clar et al [17] generated a kidney-specific *G6pc*-deficient mouse line that retained 50% of wild-type renal G6Pase-α activity. The kidney-specific *G6pc*-deficient mice survived to adulthood and presented early renal perturbations only after age 6 months [17]. Beyond age 6 months, Clar et al [17] reported that while renal levels of angiotensinogen were increased, renal levels of β-catenin were decreased and *a-SMA* mRNA levels were unchanged in these mice. Since GSD-Ia is an autosomal recessive disease, and heterozygous carriers with 50% of renal G6Pase-α activity are phenotypically normal [1–3], we sought to generate a mouse model in which kidney G6Pase-α activity was fully absent. We achieved this through a post-natal restoration of liver G6Pase-α activity in *G6pc*−/− mice using liver-directed gene augmentation therapy that does not transduce the kidney [27,28]. Our findings contrast to those of Clar et al [17]. In our fully G6Pase-αdeficient kidney models, *G6pc*−/− and K-*G6pc*−/− mice, we show that renal Wnt/β-catenin signaling is activated along with increased α-SMA.

The marked renal glycogen accumulation in *G6pc*−/− mice contributes to AKI. One strategy to prevent AKI in GSD-Ia might be to reduce renal glycogen synthesis via inhibition of glycogen synthase, the rate-limiting enzyme for glycogen biosynthesis. Indeed Tang et al [46] have developed small molecule inhibitors of glycogen synthase that may be used to treat GSD-Ia nephropathy. Another strategy is to restore gluconeogenesis, reduce glycogen storage, and normalize glucose reabsorption via *G6PC* gene transfer. We have shown that rAAV8-G6PC-mediated gene therapy corrected metabolic abnormalities associated with GSD-Ia [27]. However systemic administration of rAAV8-G6PC failed to target the kidney [28]. Rocca et al [47] have shown that retrograde renal vein injection of a rAAV9 vector efficiently targets the kidney cortex and medulla, suggesting that retrograde renal vein injection of rAAV9-G6PC may offer another way to restore renal G6Pase-α expression and correct GSD-Ia nephropathy.

In summary, we have shown that G6Pase-α-deficient kidney displays impaired gluconeogenesis, altered glucose reabsorption, elevated glycogen accumulation, and AKI. These changes are associated with activation of the Wnt/β-catenin/RAS axis along with increased expression of Dkk3 and CTGF that work with Wnt/β-catenin to promote renal fibrosis. We have also shown that ICG-001, an antagonist to Wnt/β-catenin signaling reduces renal fibrosis, offering one promising therapeutic strategy for GSD-Ia nephropathy.

Finally, we have developed and characterized a new kidney-specific *G6pc*−/− mouse model that will enable longer term studies of kidney dysfunction in GSD-Ia.

Acknowledgements

We thank the NICHD Microscopy Core and Dr. Vincent Schram for performing immunohistochemical imaging.

Funding

This work was supported by the Intramural Research Program of the *Eunice Kennedy Shriver* National Institute of Child Health and Human Development, National Institutes of Health. https://intramural.nih.gov/search/searchview.taf?ipid=126606&ts=1679692671&nidbreload=true

Data availability

Data will be made available upon request.

List of abbreviations

AGT	angiotensinogen
AKI	acute kidney injury
BUN	blood urea nitrogen
CBP	cAMP response-element binding protein binding protein
CKD	chronic kidney disease
CTGF	Connective tissue growth factor
Dkk3	Dickkopf-3
ECM	extracellular matrix
EMT	epithelial-to-mesenchymal transition
G6P	glucose-6-phosphate
G6Pase-α	glucose-6-phosphatase-α
***G6pc*−/−**	*G6pc*-deficient
GLUT	glucose transporter
GSD-I	glycogen storage disease type I
H&E	hematoxylin and eosin
K-*G6pc*−/−	kidney-specific *G6pc*-deficient
LRP5/6	low-density lipoprotein receptor-related protein-5/6
PRR	Pro-renin receptor
RAS	renin-angiotensin system

SGLT	sodium-glucose cotransporter
α-SMA	α-smooth muscle actin
TCF/LEF	T-cell factor/lymphoid enhancer-binding factor

References

[1]. Chou JY, Jun HS, Mansfield BC, Glycogen storage disease type I and G6Pase-beta deficiency: etiology and therapy. Nat. Rev. Endocrinol 6 (12) (2010) 676–688. [PubMed: 20975743]

[2]. Chou JY, Jun HS, Mansfield BC, Type I glycogen storage diseases: Disorders of the glucose-6-phosphatase/glucose-6-phosphate transporter complexes. J. Inherit. Metab. Dis 38 (3) (2015) 511–519. [PubMed: 25288127]

[3]. Kishnani PS, Austin SL, Abdenur JE, et al. , Diagnosis and management of glycogen storage disease type I: a practice guideline of the American College of Medical Genetics and Genomics. Genet. Med 16 (11) (2014) e1. [PubMed: 25356975]

[4]. Greene HL, Slonim AE, O'Neill JA Jr, et al. , Continuous nocturnal intragastric feeding for management of type 1 glycogen-storage disease. N. Engl. J. Med 294 (8) (1976) 423–425. [PubMed: 813144]

[5]. Chen YT, Cornblath M, Sidbury JB, Cornstarch therapy in type I glycogen storage disease. N. Engl. J. Med 310 (3) (1984) 171–175. [PubMed: 6581385]

[6]. Ross KM, Ferrecchia IA, Dahlberg KR, et al. , Dietary management of the glycogen storage Diseases: evolution of treatment and ongoing controversies. Adv. Nutr 11 (2) (2020) 439–446. [PubMed: 31665208]

[7]. Chen YT, Coleman RA, Scheinman JI, et al. , Renal disease in type I glycogen storage disease. N. Engl. J. Med 318 (1) (1988) 7–11. [PubMed: 3422104]

[8]. Chou JY, Mansfield BC, Weinstein DA, Renal disease in glycogen storage disease. In: Genetic Diseases of the Kidney (ed. Lifton R, Somlo S, Giebisch G, Seldon D) 695–710 (Academic Press, New York, 2008).

[9]. Liu Y, Cellular and molecular mechanisms of renal fibrosis. Nat. Rev. Nephrol 7 (12) (2011) 684–696. [PubMed: 22009250]

[10]. Humphreys BD, Mechanisms of renal fibrosis. Annu. Rev. Physiol 80 (2018) 309–326. [PubMed: 29068765]

[11]. Lei KJ, Chen H, Pan CJ, et al. , Glucose-6-phosphatase dependent substrate transport in the glycogen storage disease type 1a mouse. Nat. Genet 13 (2) (1996) 203–209. [PubMed: 8640227]

[12]. Yiu WH, Pan CJ, Ruef RA, et al. , Angiotensin mediates renal fibrosis in the nephropathy of glycogen storage disease type Ia. Kidney Internal. 73 (6) (2008) 716–723.

[13]. Zhou L, Li Y, Hao S, et al. , Multiple genes of the renin-angiotensin system are novel targets of Wnt/β-catenin signaling. J. Am. Soc. Nephrol 26 (1) (2015) 107–120. [PubMed: 25012166]

[14]. Zhou L, Liu Y, Wnt/β-catenin signaling and renin-angiotensin system in chronic kidney disease. Curr. Opin. Nephrol. Hypertens 25 (2) (2016) 100–106. [PubMed: 26808707]

[15]. Zuo Y, Liu Y, New insights into the role and mechanism of Wnt/β-catenin signaling in kidney fibrosis. Nephrology 23 (suppl 4) (2018) 38–43.

[16]. Schunk SJ, Floege J, Fliser D, et al. , WNT-β-catenin signalling - a versatile player in kidney injury and repair. Nat. Rev. Nephrol 17 (3) (2021) 172–184. [PubMed: 32989282]

[17]. Clar J, Gri B, Calderaro J, et al. , Targeted deletion of kidney glucose-6 phosphatase leads to nephropathy. Kidney Internal 86 (4) (2014) 747–756.

[18]. Gerich JE, Role of the kidney in normal glucose homeostasis and in the hyperglycemia of diabetes mellitus: therapeutic implications. Diabet. Med 27 (2) (2010) 136–42. [PubMed: 20546255]

[19]. Alsahli M, Gerich JE, Renal glucose metabolism in normal physiological conditions and in diabetes. Diabetes Res. Clin. Pract 133 (2017) 1–9. [PubMed: 28866383]

[20]. Shepard BD, Pluznick JL, Saving the sweetness: renal glucose handling in health and disease. Am. J. Physiol. Renal Physiol 313 (1) (2017) F55–F61. [PubMed: 28356283]

[21]. Ghezzi C, Loo DDF, Wright EM, Physiology of renal glucose handling via SGLT1, SGLT2 and GLUT2. Diabetologia 61 (10) (2018) 2087–2097. [PubMed: 30132032]

[22]. Vallon V, Glucose transporters in the kidney in health and disease. Pflugers Arch. 472 (9) (2020) 1345–1370. [PubMed: 32144488]

[23]. Chevalier RL, The proximal tubule is the primary target of injury and progression of kidney disease: role of the glomerulotubular junction. Am. J. Physiol. Renal Physiol 311 (1) (2016) F145–F161. [PubMed: 27194714]

[24]. Hao S, He W, Li Y, et al. , Targeted inhibition of β-catenin/CBP signaling ameliorates renal interstitial fibrosis. J. Am. Soc. Nephrol 22 (9) (2011) 1642–653. [PubMed: 21816937]

[25]. Voronkov A, Kraus S, Wnt/beta-catenin signaling and small molecule inhibitors. Curr. Pharm. Des 19 (4) (2013) 634–664. [PubMed: 23016862]

[26]. Kahn M, Taking the road less traveled - the therapeutic potential of CBP/β-catenin antagonists. Expert Opin. Ther. Targets 25 (9) (2021) 701–719. [PubMed: 34633266]

[27]. Yiu WH, Lee YM, Peng WT, et al. , Complete normalization of hepatic G6PC deficiency in murine glycogen storage disease type Ia using gene therapy. Mol. Ther 18 (6) (2010) 1076–1084. [PubMed: 20389290]

[28]. Lee YM, Pan CJ, Koeberl DD, et al. , The Upstream enhancer elements of the *G6PC* promoter are critical for optimal G6PC expression in murine glycogen storage disease type Ia. Mol. Genet. Metab 110 (3) (2013) 275–280. [PubMed: 23856420]

[29]. Cho JH, Kim GY, Mansfield BC, et al. , Hepatic glucose-6-phosphatase-α deficiency leads to metabolic reprogramming in glycogen storage disease type Ia. Biochem. Biophys. Res. Commun 498 (2) (2018) 925–931. [PubMed: 29545180]

[30]. Gowda S, Desai PB, Kulkarni SS, et al. , Markers of renal function tests. N. Am. J. Med. Sci 2 (4) (2010) 170–173.

[31]. Nürnberger J, Feldkamp T, Kavapurackal R, et al. , N-cadherin is depleted from proximal tubules in experimental and human acute kidney injury. Histochem. Cell Biol 133 (6) (2010) 641–649. [PubMed: 20440507]

[32]. Fang X, Hu J, Chen Y, et al. , Dickkopf-3: Current Knowledge in Kidney Diseases. Front. Physiol 11 (2020) 533344. [PubMed: 33391006]

[33]. Li Z, Zhou L, Wang Y, et al. , (Pro)renin receptor is an amplifier of Wnt/β-catenin signaling in kidney injury and fibrosis. J. Am. Soc. Nephrol 28 (8) (2017) 2393–2408. [PubMed: 28270411]

[34]. Ichihara A, Yatabe MS, The (pro)renin receptor in health and disease. Nat. Rev. Nephrol 15 (11) (2019) 693–712. [PubMed: 31164719]

[35]. Ramazani Y, Knops N, Elmonem MA, et al. , Connective tissue growth factor (CTGF) from basics to clinics. Matrix Biol. 68-69 (2018) 44–66. [PubMed: 29574063]

[36]. Yin Q, Liu H, Connective Tissue Growth Factor and Renal Fibrosis. Adv. Exp. Med. Biol 1165 (2019) 365–380. [PubMed: 31399974]

[37]. Yang T, Xu C, Physiology and pathophysiology of the intrarenal renin-angiotensin system: an update. J. Am. Soc. Nephrol 28 (4) (2017) 1040–1049. [PubMed: 28255001]

[38]. Grande MT, Sánchez-Laorden B, López-Blau C, et al. , Snail1-induced partial epithelial-to-mesenchymal transition drives renal fibrosis in mice and can be targeted to reverse established disease. Nat. Med 21 (9) (2015) 989–997. [PubMed: 26236989]

[39]. Klingberg F, Hinz B, White ES, The myofibroblast matrix: implications for tissue repair and fibrosis. J. Pathol 229 (2) (2013) 298–309. [PubMed: 22996908]

[40]. Bülow RD, Boor P. Extracellular matrix in kidney fibrosis: more than just a scaffold. J. Histochem. Cytochem 67 (9) (2019) 643–661. [PubMed: 31116062]

[41]. Rieg T A high-throughput method for measurement of glomerular filtration rate in conscious mice. J. Vis. Exp 75 (2013) e50330.

[42]. Hosten AO, BUN and Creatinine, In: Walker HK, Hall WD, Hurst JW (Eds). Clinical Methods: The History, Physical, and Laboratory Examinations. 3rd edition. Butterworths, Boston, 1990. Chapter 193.

[43]. Rooney B, O'Donovan H, Gaffney A, et al. , CTGF/CCN2 activates canonical Wnt signalling in mesangial cells through LRP6: implications for the pathogenesis of diabetic nephropathy. FEBS Lett. 585 (3) (2011) 531–538. [PubMed: 21237163]

[44]. Melis D, Parenti G, Gatti R, et al. , Efficacy of ACE-inhibitor therapy on renal disease in glycogen storage disease type 1: a multicentre retrospective study. Clin. Endocrinol. (Oxf) 63 (1) (2005) 19–25. [PubMed: 15963056]

[45]. Martens DH, Rake JP, Navis G, et al. , Renal function in glycogen storage disease type I, natural course, and renopreservative effects of ACE inhibition. Clin. J. Am. Soc. Nephrol (11) (2009) 1741–1746. [PubMed: 19808227]

[46]. Tang B, Frasinyuk MS, Chikwana VM, et al. , Discovery and Development of Small-Molecule Inhibitors of Glycogen Synthase. J. Med. Chem 63 (7) (2020) 3538–3551. [PubMed: 32134266]

[47]. Rocca CJ, Ur SN, Harrison F, et al. , rAAV9 combined with renal vein injection is optimal for kidney-targeted gene delivery: conclusion of a comparative study. Gene Ther. 21 (6) (2014) 618–628. [PubMed: 24784447]

[48]. Bankhead P, Loughrey MB, Fernández JA, et al. , QuPath: Open source software for digital pathology image analysis. Sci. Rep 7 (1) (2017) 16878. [PubMed: 29203879]

Lee et al Highlights

- GSD-Ia mice display acute kidney injury.
- GSD-Ia nephropathy is caused, in part, by activation of Wnt/β-catenin signaling.
- Drug inhibition of the Wnt/β-catenin pathway reduces renal fibrosis in GSD-Ia.

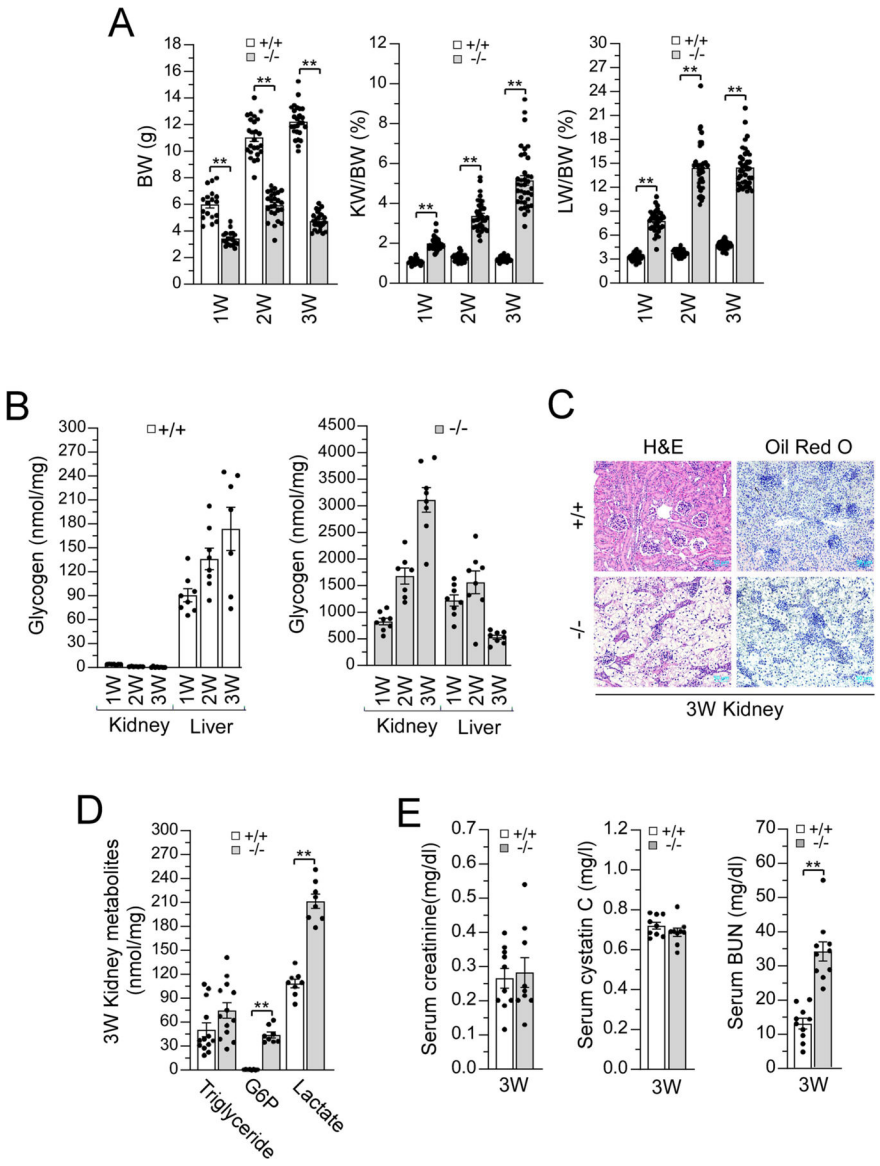

Fig. 1.

G6pc−/− mice display metabolic abnormalities during post-natal development. (A) Changes in body weight (BW), the ratios of kidney weight (KW) to BW, and the ratios of liver weight (LW) to BW in control (n ≥18) and *G6pc*−/− (n ≥18) mice. (B) Renal and hepatic levels of glycogen in control (n = 6–8 for each group) and *G6pc*−/− mice (n = 6–8 for each group). Note the 15-fold change in y-axis scale. (C) H&E and Oil Red O (neutral triglycerides and lipids) staining of the kidneys in 3-week-old control and *G6pc*−/− mice. Scale bar, 50 μm. (D) Renal levels of G6P, lactate and triglyceride in 3-week-old control (n = 6–16) and *G6pc*−/− (n = 6–16) mice. (E) Serum levels of creatinine, cystatin C, and BUN in 3-week-old control (n = 9–10) and *G6pc*−/− (n = 9–10) mice. Values represent the mean ± SEM. **P* < 0.05, ***P* < 0.01.

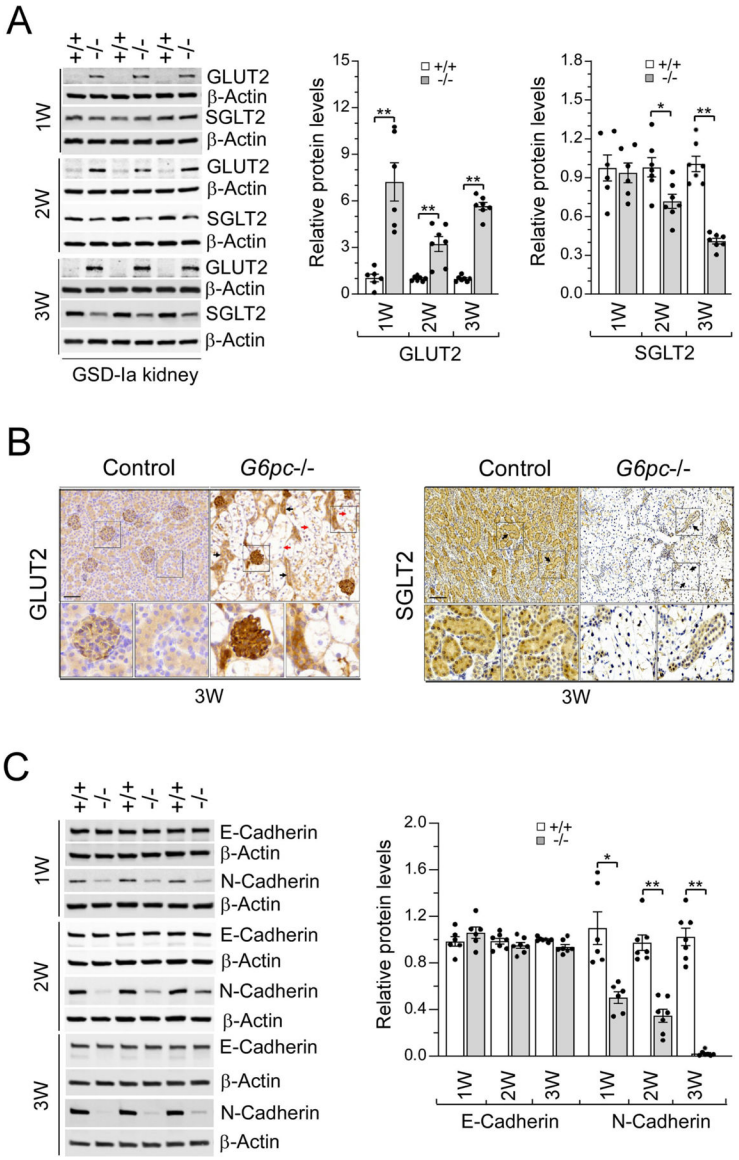

Fig. 2.

G6pc−/− mice display altered renal glucose reabsorption and reduced expression of N-cadherin during postnatal development. (A) Western-blot analyses and quantitation of renal levels of GLUT2 and SGLT2 in control (n = 6 per group) and *G6pc*−/− (n = 6 per group) mice. (B) Immunohistochemical analysis of GLUT2 and SGLT2 in the kidneys of 3-week-old control and *G6pc*−/− mice. Scale bar, 50 μm. (C) Western-blot analyses and quantitation of renal levels of E-cadherin and N-cadherin in control (n = 6 per group) and *G6pc*−/− (n = 6 per group) mice. Three sets of representative immune-stained lanes for controls (+/+) and *G6pc*−/− (−/−) mice are shown for each protein. Densitometric quantification was performed and normalized against β-actin. Values represent the mean ± SEM. **P* < 0.05, ***P* < 0.01.

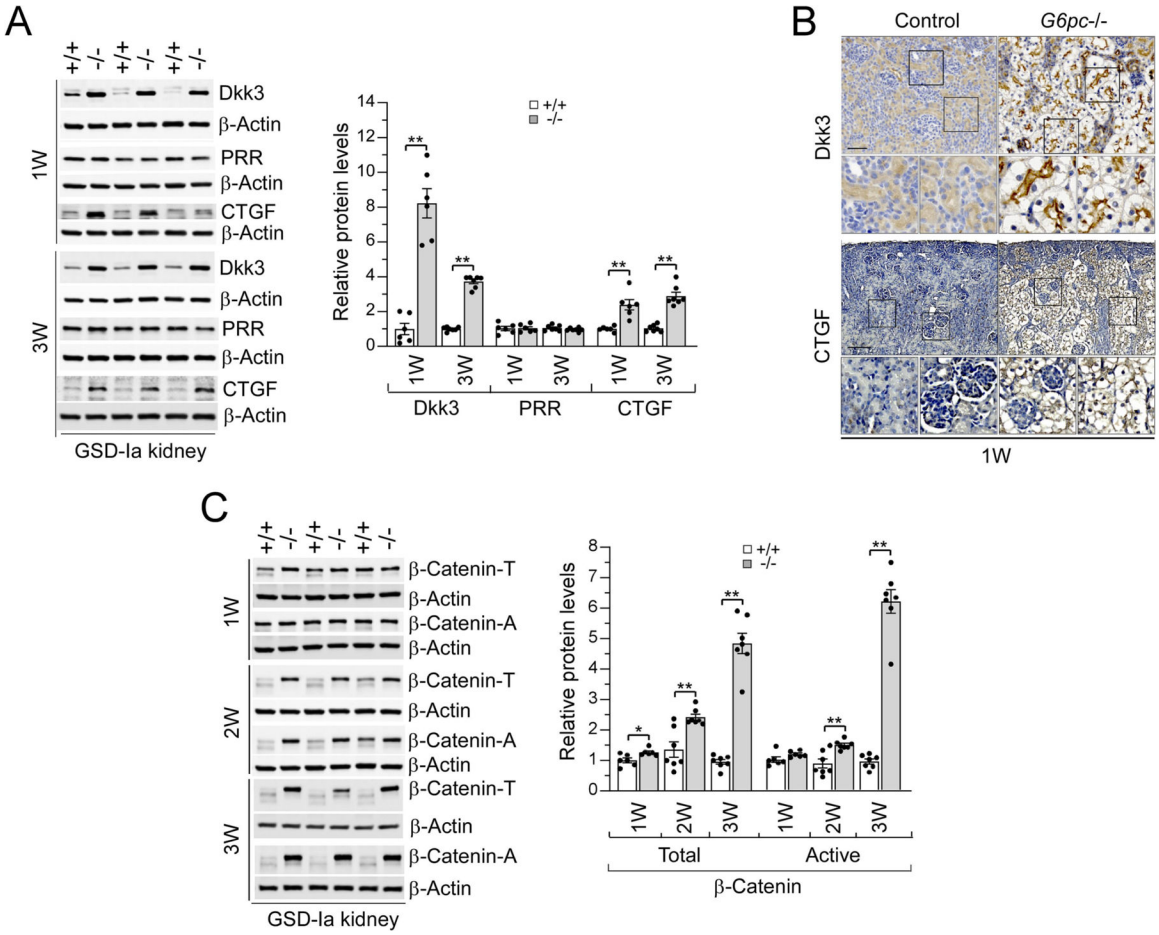

Fig. 3.

Renal levels of Dkk3, PRR, CTGF, and β-catenin in *G6pc*−/− mice during postnatal development. (A) Western-blot analyses and quantitation of renal levels of Dkk3, PRR and CTGF in control (n = 6 per group) and *G6pc*−/− (n = 6 per group) mice. (B) Immunohistochemical analysis of Dkk3 and CTGF in the kidneys of 1-week-old control and *G6pc*−/− mice. Scale bar, 50 μm. (C) Western-blot analyses and quantitation of renal levels of total (β-catenin-T) and active, dephosphorylated (β-catenin-A) β-catenin in control (n = 6 per group) and *G6pc*−/− (n = 6 per group) mice. Three sets of representative immune-stained lanes for controls (+/+) and *G6pc*−/− (−/−) mice are shown for each protein. Densitometric quantification was performed and normalized against β-actin. Values represent the mean ± SEM. **P* < 0.05,

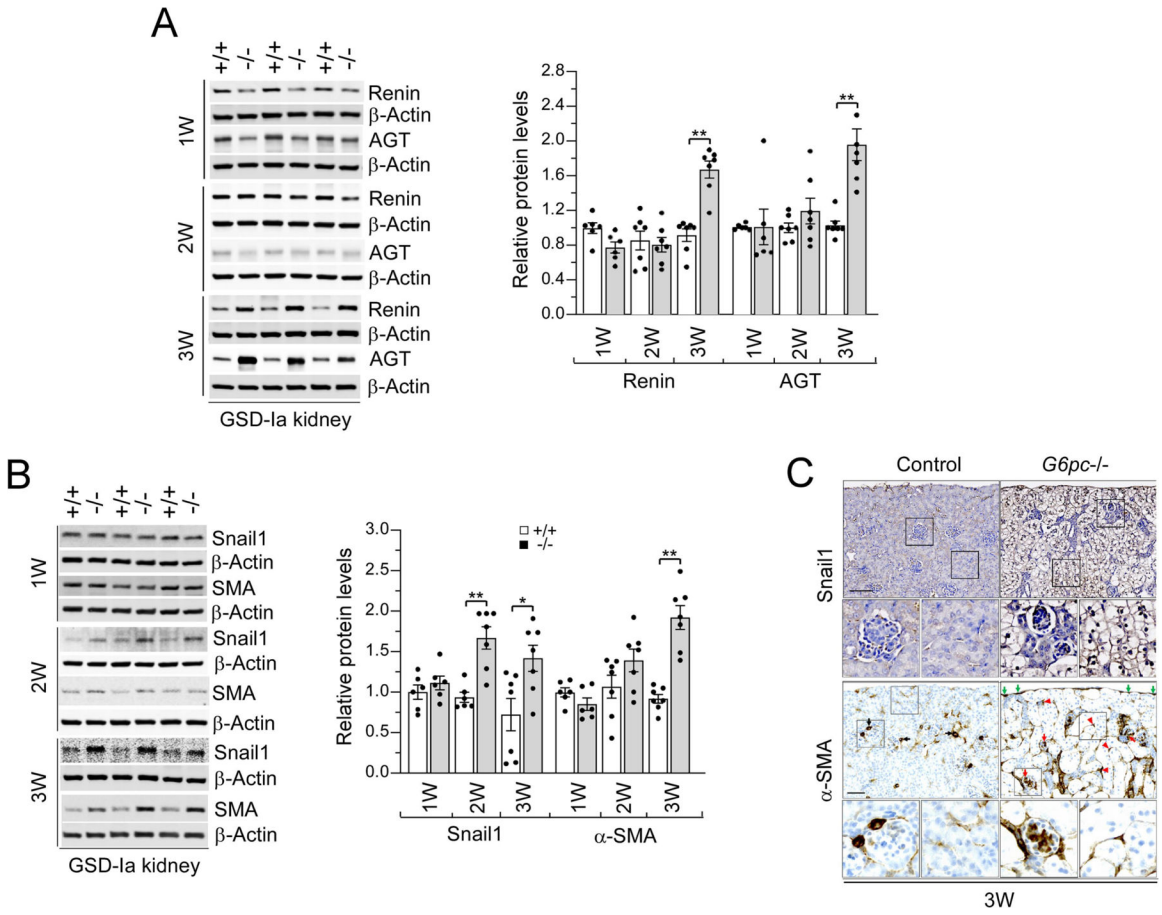

Fig. 4.

G6pc−/− mice display increased renal levels of renin, AGT, Snail1, and α-SMA during postnatal development. (A) Western-blot analyses and quantification of renal levels of renin and AGT in control (n = 6 per group) and *G6pc*−/− (n = 6 per group) mice. (B) Western-blot analyses and quantification of renal levels of Snail1 and α-SMA in control (n = 6 per group) and *G6pc*−/− (n = 6 per group) mice. Three sets of representative immune-stained lanes for controls (+/+) and *G6pc*−/− (−/−) mice are shown for each protein. Densitometric quantification was performed and normalized against β-actin. Values represent the mean ± SEM. **P* < 0.05, ***P* < 0.01. (C) Immunohistochemical analysis of Snail1 and α-SMA in the kidneys of 3-week-old control and *G6pc*−/− mice. Scale bar, 50 μm.

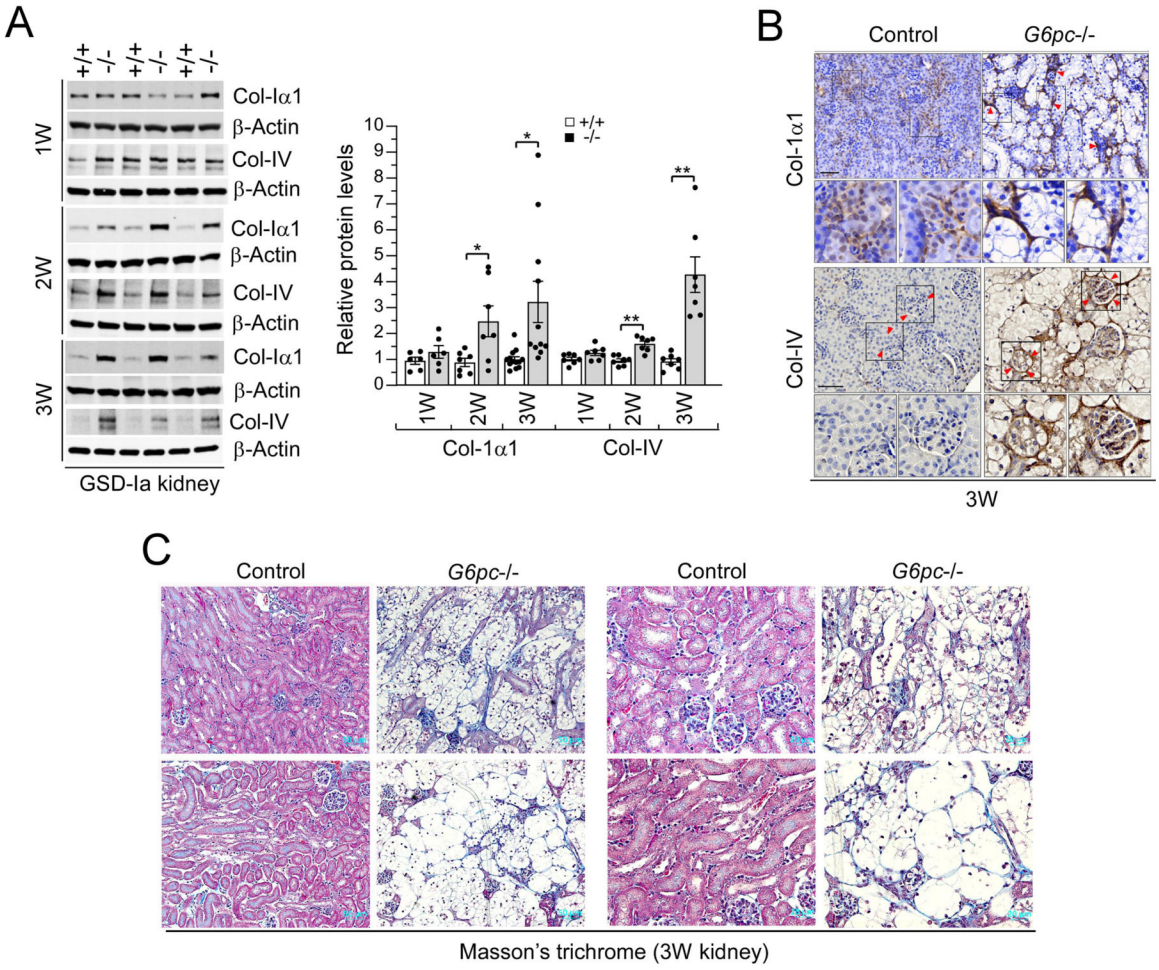

Fig. 5.

G6pc−/− mice display increased renal levels Col-1αI and Col-IV, and renal fibrosis. (A) Western-blot analyses and quantification of renal levels of Col-1αI and Col-IV in control (n = 6 per group) and *G6pc*−/− (n = 6 per group) mice during the weeks 1 to 3 postnatal development. Three sets of representative immune-stained lanes for controls (+/+) and *G6pc*−/− (−/−) mice are shown for each protein. Densitometric quantification was performed and normalized against β-actin. Values represent the mean ± SEM. **P* < 0.05, ***P* < 0.01. (B) Immunohistochemical analysis of Col-1αI and Col-IV in the kidneys of 3-week-old control and *G6pc*−/− mice. Scale bar, 50 μm. (C) Masson's trichrome staining of kidney sections in 3-week-old control and *G6pc*−/− mice at magnifications of x200 (left panels, Scale bar, 50 μm) and x400 (right panels, Scale bar, 20 μm). Renal fibrosis in *G6pc*−/− mice was shown by the blue colored staining of the collagen fibers.

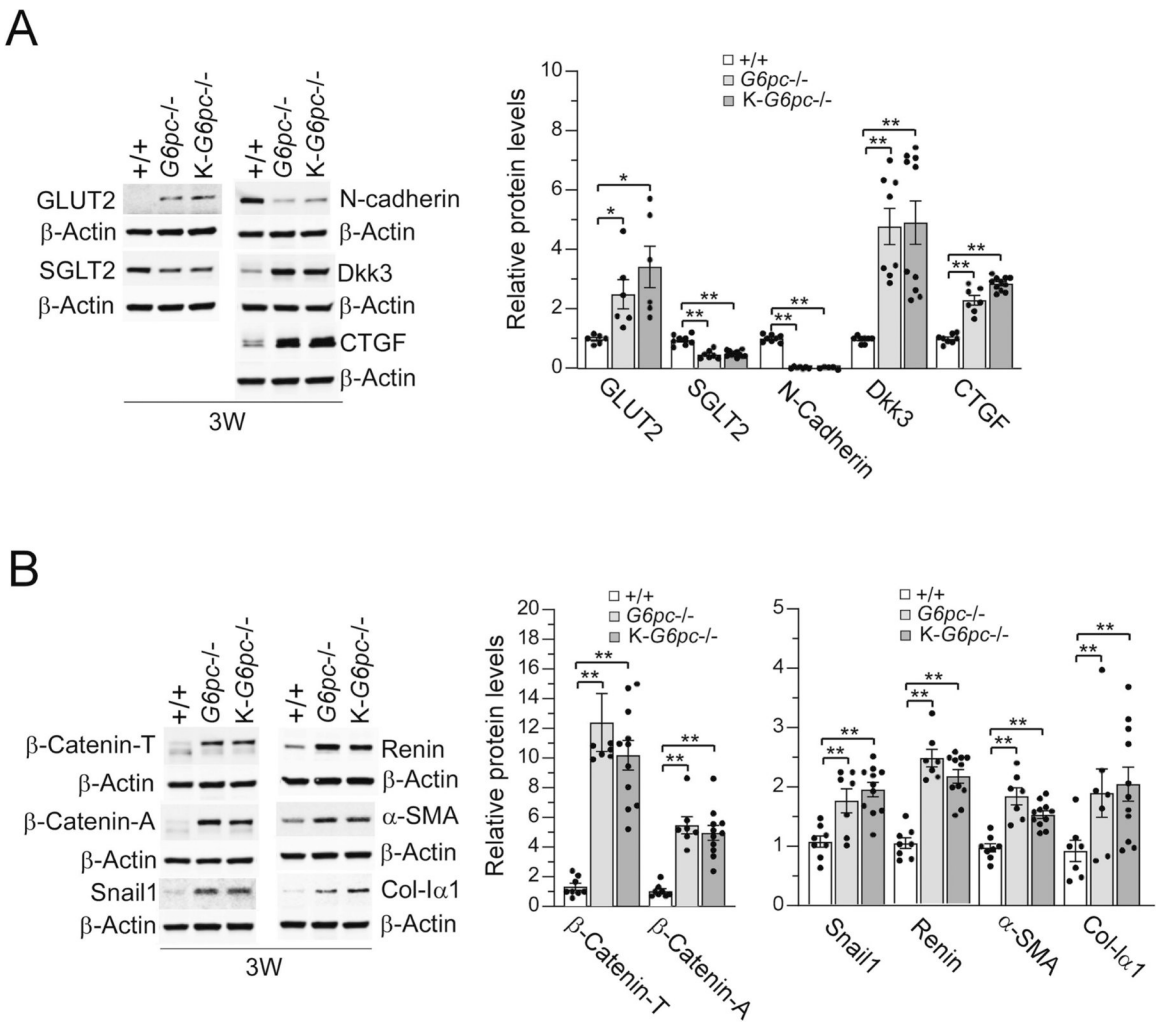

Fig. 6.

G6pc−/− and K-G6pc−/− mice display similar renal phenotype. The K-*G6pc*−/− mice were generated by treating 2-day-old *G6pc*−/− mice with 1×10^{12} vg/kg of rAAV8-G6PC [27] that target the liver but not the kidneys [28]. The resulting K-*G6pc*−/− mice restored low levels of liver G6Pase-α activity but lacked renal G6Pase-α expression survived to adulthood, while expressing an abnormal kidney phenotype mimicking the *G6pc*−/− mice. (A) Western-blot and quantification analyses of renal levels of GLUT2, SGLT2, N-cadherin, Dkk3, and CTGF in 3-week-old control (+/+; n = 6), *G6pc*−/− (n = 6) and K-*G6pc*−/− (n = 6) mice. (B) Western-blot and quantification analyses of renal levels of β-catenin, Snail1, renin, α-SMA, and Col-1αI in 3-week-old control (n = 6), *G6pc*−/− (n = 6) and K-*G6pc*−/− (n = 6) mice. Representative immune-stained lanes for these mice are shown for each protein. Densitometric quantification was performed and normalized against β-actin. Values represent the mean ± SEM. *$P < 0.05$, **$P < 0.01$.

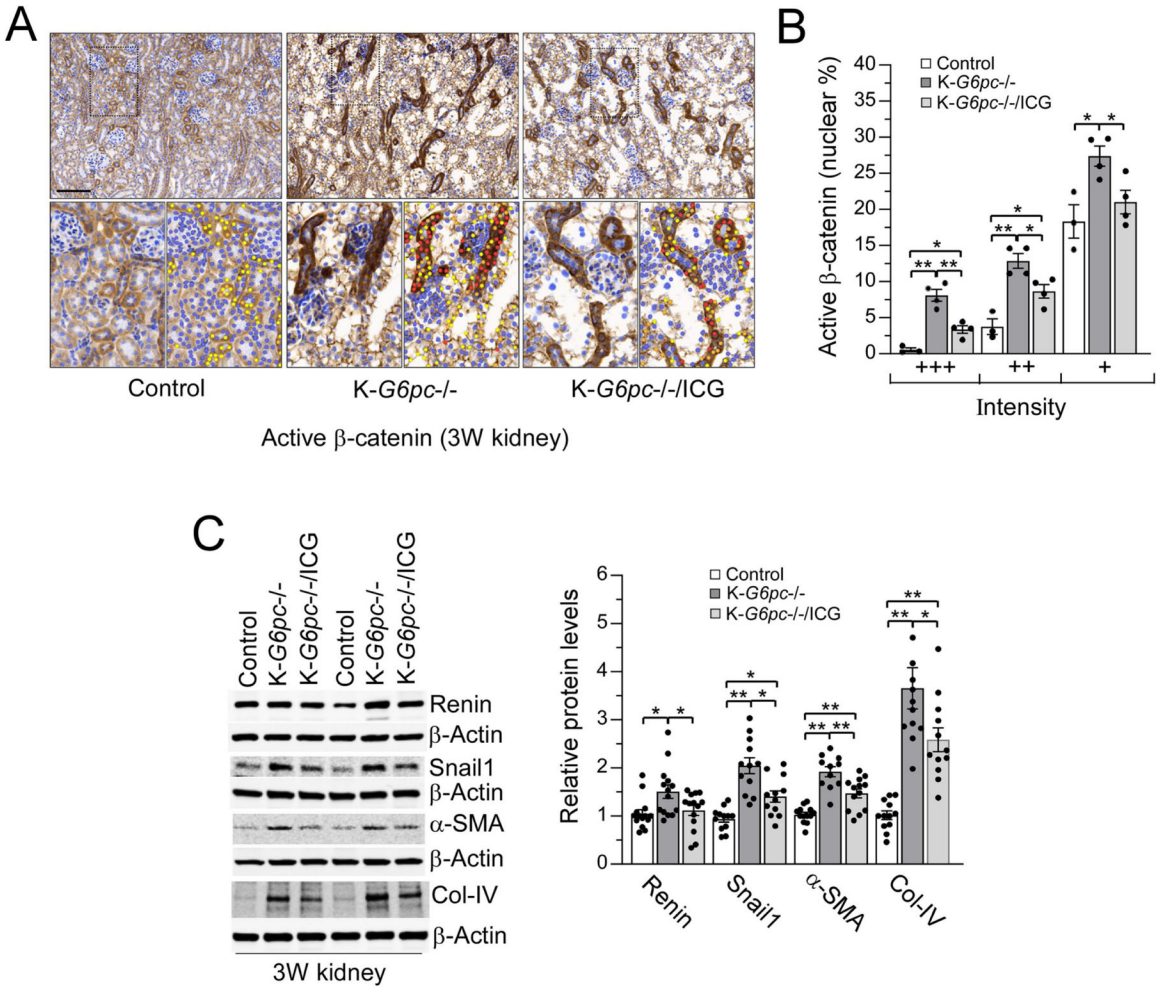

Fig. 7.

ICG-001 Inhibited Wnt/*β*-catenin signaling and reduced renal fibrosis. Three-day-old K-*G6pc*−/− mice were treated with ICG-001 at 500 μg/day, via intraperitoneal injection, for 18 consecutive days and the expression of active nuclear translocated β-catenin and the target genes was examined in 3-week-old control (n = 10–12 per group), K-*G6pc*−/− (n = 10–12 per group) and ICG-001-treated K-*G6pc*−/− (K-*G6pc*−/−/ICG; n = 10–12 per group) mice. (A) Immunohistochemical analysis of renal levels of active β-catenin. Scale bar, 50 μm. (B) Quantification of renal levels of active β-catenin. Kidney sections were digitalized using Motic EasyScan Infinity 60 (Motic Digital Pathology, Emeryville, CA, USA), then analyzed by QuPath software v0.3.2 (Edinburgh, UK). Multiple annotations were selected on the entire renal cortex. The nucleus DAB OD mean scoring [48] identified three optical density thresholds for the nuclear stained β-catenin: negative (blue dots), weak (+, yellow dots), moderate (++, orange dots), and strong (+++, red dots). (C) Western-blot analyses and quantification of renal levels of renin, Snail1, α-SMA and Col-IV. Two sets of representative immune-stained lanes are shown for each protein. Densitometric quantification was performed and normalized against β-actin. Values represent the mean ± SEM. **P* < 0.05, ***P* < 0.01.

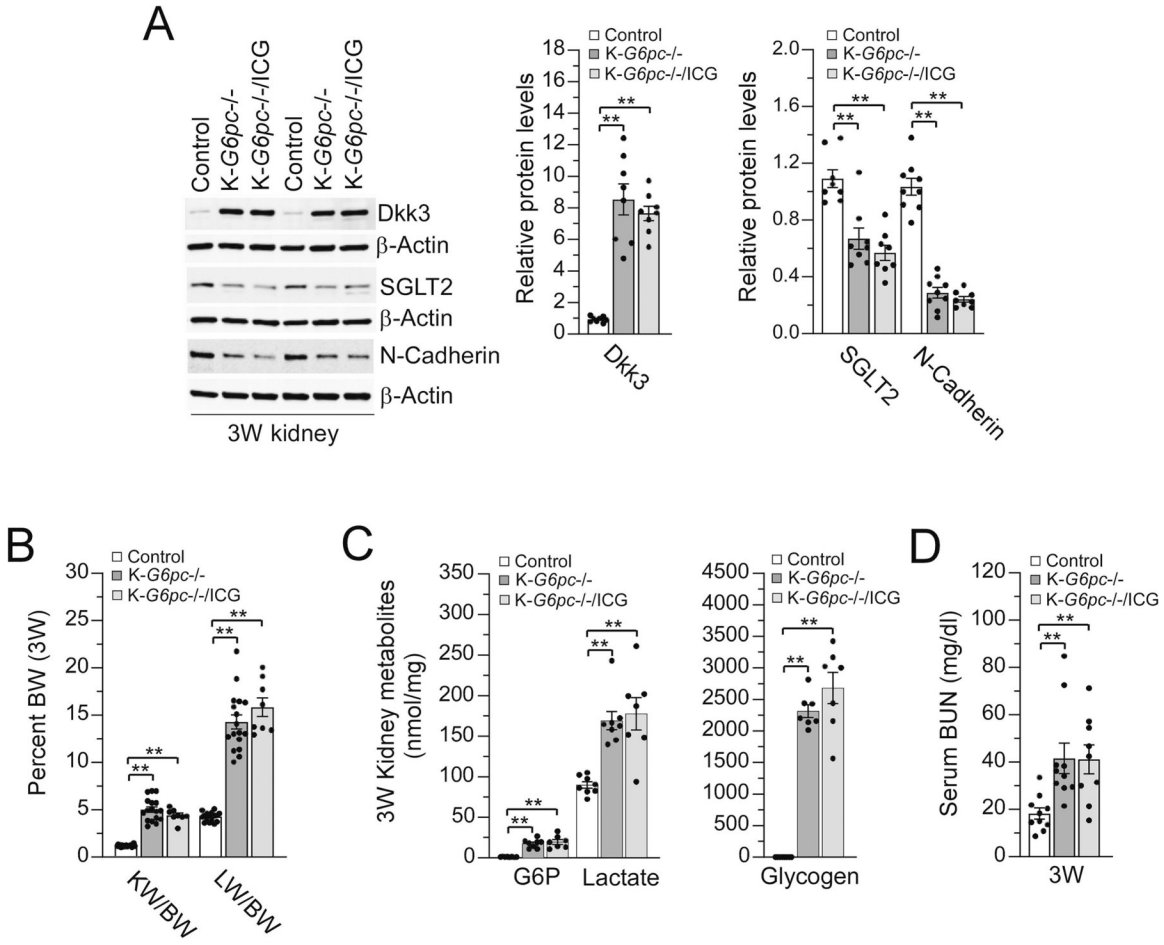

Fig. 8.

Effects of ICG-001 on renal levels of Dkk3, SGLT2, N-cadherin, nephromegaly, hepatomegaly, renal levels of G6P, lactate, glycogen as well as serum levels of BUN. Three-day-old K-*G6pc*−/− mice were treated with ICG-001 at 500 μg/day, via intraperitoneal injection, for 18 consecutive days to age 3 weeks. Renal levels of Dkk3, SGLT2, N-cadherin, nephromegaly, hepatomegaly, renal levels of metabolites, and serum levels of BUN were examined in 3-week-old control (n = 9–10 per group), K-*G6pc*−/− (n = 9–10 per group) and ICG-001-treated K-*G6pc*−/− (K-*G6pc*−/−/ICG; n = 9–10 per group) mice. (A) Western-blot analyses and quantification of renal levels of Dkk3, SGLT2, and N-cadherin. Two sets of representative immune-stained lanes are shown for each protein. Densitometric quantification was performed and normalized against β-actin. (B) The ratios of KW to BW and LW to BW. (C) Renal levels of G6P, lactate and glycogen. (D) Serum levels of BUN. Values represent the mean ± SEM. $^{**}P < 0.01$.